Ozols, J., Carr, S. A., & Strittmatter, P. (1984) *J. Biol. Chem. 259*, 13349-13354.
Pellman, D., Garber, E. A., Cross, F. R., & Hanafusa, H. (1985a) *Nature (London) 314*, 374-377.
Pellman, D., Garber, E. A., Cross, F. R., & Hanafusa, H. (1985b) *Proc. Natl. Acad. Sci. U.S.A. 82*, 1623-1627.
Quinn, P., Griffiths, G., & Warren, G. (1983) *J. Cell Biol. 96*, 851-856.
Schmidt, M. F. G. (1983) *Curr. Top. Microbiol. Immunol. 102*, 101-124.
Schmidt, M. F. G., & Schlesinger, M. J. (1979) *Cell (Cambridge, Mass.) 17*, 813-819.
Schmidt, M. F. G., & Schlesinger, M. J. (1980) *J. Biol. Chem. 255*, 3334-3339.
Schmidt, M. F. G., Bracha, M., & Schlesinger, M. J. (1979) *Proc. Natl. Acad. Sci. U.S.A. 76*, 1687-1691.
Schubert, D., Harris, A. J., Devine, C. E., & Heinemann, S. (1974) *J. Cell Biol. 61*, 398-413.
Schultz, A. M., Henderson, L. E., Oroszlan, S., Garber, E. A., & Hanafusa, H. (1985) *Science (Washington, D.C.) 227*, 427-429.
Sefton, B. M., Trowbridge, I. S., Cooper, J. A., & Scolnick, E. M. (1982) *Cell (Cambridge, Mass.) 31*, 465-474.
Staufenbiel, M., & Lazarides, E. (1986) *Proc. Natl. Acad. Sci. U.S.A. 83*, 318-322.
Towler, D., & Glaser, L. (1986) *Biochemistry 25*, 878-884.
Willumsen, B. M., Christensen, A., Hubbert, N. L., Papageorge, A. G., & Lowy, D. R. (1984) *Nature (London) 310*, 583-586.

Scanning Calorimetric Study of Fully Hydrated Asymmetric Phosphatidylcholines with One Acyl Chain Twice as Long as the Other†

Hui Xu and Ching-hsien Huang*

Department of Biochemistry, University of Virginia School of Medicine, Charlottesville, Virginia 22908

Received September 19, 1986; Revised Manuscript Received October 30, 1986

ABSTRACT: The asymmetric C(18):C(10)PC molecules are known by X-ray diffraction to self-assemble, in excess water, into a lamellar structure known as the mixed interdigitated bilayer at $T < T_m$. In this structure, the long C(18)-acyl chain is interdigitated fully across the entire hydrocarbon width of the bilayer, while the shorter C(10)-acyl chain, which is about half as long as the C(18)-acyl chain, packs end to end with a C(10)-acyl chain of another lipid molecule in the opposing bilayer leaflet. We have synthesized the following asymmetric phosphatidylcholines (PC's): C(16):C(9)PC, C(16):C(10)PC, C(18):C(10)PC, C(18):C(11)PC, C(20):C(11)PC, C(20):C(12)PC, C(22):C(12)PC, C(22):C(13)PC, C(8):C(18)PC, and C(10):C(22)PC. These 10 asymmetric phosphatidylcholines have a common characteristic; i.e., the length of the longer extended acyl chain is about twice as long as that of the shorter acyl chain. On the basis of the known lamellar structure of C(18):C(10)PC, we anticipate that these asymmetric phosphatidylcholines will also form mixed interdigitated bilayers. We have employed high-resolution differential scanning calorimetry (DSC) to investigate the thermotropic behavior of liposomes prepared from these asymmetric phosphatidylcholines. If our anticipation is correct, one would find that the thermodynamic data (T_m, ΔH, or ΔS) associated with the main thermal phase transitions of these asymmetric phosphatidylcholine dispersions will fit into a continuous curve as they are plotted as a function of the hydrocarbon width of the putative mixed interdigitated bilayer. Experimental data presented in this paper indeed bear this out. For comparison, a DSC study of multilamellar dispersions prepared from a series of saturated symmetric phosphatidylcholines has also been carried out. The thermodynamic data associated with the main phase transition of these symmetric phosphatidylcholine dispersions are shown to be distinctively different from those of asymmetric phosphatidylcholine species with the same molecular weight. Saturated symmetric phosphatidylcholines are well-known to form normal noninterdigitated bilayers in excess water. When thermodynamic data are plotted against the hydrocarbon width of the normal bilayer, they all fall on a smooth continuous curve. This curve, however, is distinctively different from that fitted by the corresponding data derived from liposomes of asymmetric phosphatidylcholines. Our results can thus be taken as strong evidence to argue for the formation of mixed interdigitated bilayers by the asymmetric phosphatidylcholines under study.

Recently, considerable interest has been placed on phospholipids which, under appropriate conditions, self-assemble into interdigitated bilayers as revealed by the X-ray diffraction technique (Ranck et al., 1977; Hauser et al., 1980; Ranck & Tocanne, 1982; McDaniel et al., 1983; Serrallalch et al., 1983; McIntosh et al., 1984; Hui et al., 1984; Jain et al., 1985; Ruocco et al., 1985; Hui & Huang, 1986; Pascher & Sundell, 1986; Pascher et al., 1986). Among the various interdigitated bilayers, the mixed interdigitated packing model is perhaps most unique, since the acyl chains in the bilayer core are observed to be interdigitated in both the gel and the liquid-crystalline state (McIntosh et al., 1984; Hui et al., 1984).

† This investigation was supported, in part, by NIH Grant GM-17452 from the U.S. Public Health Service.
* Address correspondence to this author.

0006-2960/87/0426-1036$01.50/0

Asymmetric mixed-chain C(18):C(10)PC[1] serves as an example of the phospholipid species which spontaneously assembles into the mixed interdigitated bilayer in excess water. At $T < T_m$, the long hydrocarbon chain of C(18):C(10)PC is interdigitated fully across the entire hydrocarbon width of the bilayer, while the short *sn*-2 acyl chain packs end to end with the short *sn*-2 acyl chain of another lipid molecule in the opposing bilayer leaflet. The mixed interdigitated gel bilayer is thus characterized by having the area per phospholipid molecule at the lipid/water interface encompass three hydrocarbon chains, in contrast to the two and the four hydrocarbon chains per lipid head group for diacyl phospholipids in the noninterdigitated bilayer and the fully interdigitated bilayer, respectively.

Because of the characteristic packing mode observed for phospholipid acyl chains in the C(18):C(10)PC bilayer at $T < T_m$, it is suggested that only asymmetric phospholipids with very stringent chain-length differences between the *sn*-1 and *sn*-2 acyl chains can assemble into this type of mixed interdigitated bilayer (McIntosh et al., 1984; Hui et al., 1984). Specifically, it is proposed that the mixed interdigitated bilayer occurs when the chain-length difference between the *sn*-1 and *sn*-2 acyl chains (ΔC) is about half as long as the length of the longer acyl chain (CL), or the value of normalized chain-length difference ($\Delta C/CL$) is about 0.5. In calculating the chain-length difference, the apparent length of the *sn*-2 acyl chain in the gel-state bilayer is taken to be 1.5 C–C bond lengths shorter than the total length of the chain in a nearly all-trans conformation (Mason & Huang, 1981; Mason et al., 1981); this reduction is due to an abrupt *sn*-2 chain bend at the C(2) atom near the glycerol backbone region (Zaccai et al., 1979).

In an effort to demonstrate that various asymmetric phospholipids with the ratio of $\Delta C/CL$ in the neighborhood of 0.5 can form mixed interdigitated bilayers, we have first synthesized a series of phospholipids with known ratios of $\Delta C/CL$. We have then examined their thermotropic phase behavior by high-resolution differential scanning calorimetry (DSC). Our investigation shows that the thermotropic properties of multilamellar liposomes composed of pure asymmetric phospholipids with $\Delta C/CL \simeq 0.5$ are distinctively different from those of symmetric phospholipids known to form the normal bilayer with two acyl chains per lipid head group. On the basis of X-ray diffraction data of C(18):C(10)PC lamellae and the nature of phase transitions, it is concluded that different asymmetric phosphatidylcholines with $\Delta C/CL \simeq 0.5$ can indeed self-assemble to form mixed interdigitated bilayers at $T < T_m$.

Materials and Methods

All symmetric phosphatidylcholines and lysophosphatidylcholines with at least 99 mol % purity were purchased from Avanti Polar Lipids, Inc. (Birmingham, AL). All fatty acid anhydrides with purity greater than 99% were obtained from Nu Chek Prep, Inc. (Elysian, MN). High-purity (≥98 mol %) samples of mixed-chain asymmetric phosphatidylcholines such as C(16):C(9)PC, C(16):C(10)PC, C(18):C(10)PC, C(18):C(11)PC, C(20):C(11)PC, C(20):C(12)PC, C(22):C(12)PC, C(22):C(13)PC, C(8):C(18)PC, and C(10):C(22)PC were synthesized by reacylation of a 1-acyllysophosphatidylcholine of known chain length with the anhydride of the fatty acid desired to be in the 2-acyl position of the mixed-chain product. The reacylation reaction was performed in dry, ethanol-free chloroform at room temperature, employing the catalyst 4-pyrrolidinopyridine. The resulting mixed-chain asymmetric phosphatidylcholine was then purified by elution from a silicic acid column, employing a gradient of chloroform and methanol. Finally, the phosphatidylcholine was recrystallized from acetone–chloroform (95:5). After drying, the white precipitates were dispersed in a minimum volume of dry benzene and lyophilized overnight. The lyophilized sample was stored desiccated at −20 °C. The detailed method employed for the synthesis of asymmetric phosphatidylcholines has been published elsewhere (Mason et al., 1981).

Sample Preparation. In general, a fixed volume of 50 mM NaCl aqueous solution (0 °C) containing 5 mM phosphate buffer and 1 mM EDTA at pH 7.4 was added to a preweighed lyophilized phospholipid to give lipid concentrations in the range of 2–4 mM, followed by vortexing at 0 °C for 1 min. Two types of lipid preparations were used for DSC studies. The cold lipid dispersions that have not been heated above T_m are termed nonhydrated samples, a term adapted from Chowdhry et al. (1984). The second type is termed the hydrated sample which was prepared as follows. The aqueous lipid dispersion was first heated to 15 °C above T_m and was immediately vortexed at the elevated temperature for 5 min. The sample was then allowed to anneal at 0 °C for 1 h. After the freeze–thaw cycle had been repeated 2 more times, the sample was stored at 0 °C for a desired time before being loaded into the sample cell of the calorimeter which had been thermally equilibrated at a desired temperature.

Calorimetry. A high-resolution MC-2 scanning microcalorimeter (Microcal Co., Amherst, MA) equipped with the DA-2 digital data acquisition system was employed for studying the thermotropic phase behavior of the various phospholipid–water systems. Prior to use, the nonhydrated sample was degassed under vacuum, at 0 °C, and a total volume of about 1.2 mL was loaded into the calorimeter cell. The DSC traces were recorded during heating of the samples, and the scan rate was set at 10 °C/h for all phosphatidylcholine samples. The transition temperatures (T_m) were determined from the transition peaks at the maximal excess heat capacity; calorimetric enthalpies of the transitions (ΔH) were calculated from the peak areas by using software provided by Microcal Co. For hydrated samples, the degassed lipid dispersion was first incubated in the calorimeter cell at a temperature 15–20 °C below T_m. The sample was subsequently scanned at 10 °C/h in an ascending-temperature mode, and the scan was then terminated about 10 °C above T_m.

Results

Thermotropic Phase Behavior of Asymmetric Phosphatidylcholines with $\Delta C/CL = 0.50$. We have obtained heating thermograms for hydrated and nonhydrated samples of C(16):C(10)PC, C(18):C(11)PC, C(20):C(12)PC, and C(22):C(13)PC in excess water (Figure 1). This series of asymmetric phosphatidylcholines is characterized by having a common value (0.50) of $\Delta C/CL$; i.e., the apparent length of the *sn*-2 acyl chain is precisely half as long as that of the *sn*-1 acyl chain in an all-trans conformation. Within the temperature range of 0–50 °C, a single slightly asymmetric transition peak was detected by DSC for samples prepared from this series of phospholipids (Figure 1). Moreover, this single endothermic transition is highly reproducible; hydrated samples with various incubation times at 0 °C exhibit the calorimetric thermograms which are virtually indistinguishable

[1] Abbreviations: C(X):C(Y)PC, saturated L-α-phosphatidylcholine having X carbons in the *sn*-1 acyl chain and Y carbons in the *sn*-2 acyl chain; DSC, differential scanning calorimetry; EDTA, ethylenediaminetetraacetic acid.

Table I: Phase Transition Properties of Asymmetric Phosphatidylcholine Liposomes[a]

phosphatidylcholine	mol wt	T_o (°C)	T_c (°C)	T_m (°C)	$\Delta T_{1/2}$ (°C)	ΔH (kcal/mol)	ΔS (eu/mol)
C(16):C(9)PC	635.9	3.2	4.6	3.6	0.38	6.1	21.9
C(16):C(10)PC	649.9	3.3	5.3	4.9	0.23	6.5	23.2
C(18):C(10)PC	678.0	16.9	20.6	19.2	0.63	8.9	30.3
C(18):C(11)PC	692.0	19.0	21.6	21.3	0.34	9.2	31.3
C(20):C(11)PC	720.1	30.7	24.2	33.2	0.97	11.3	36.8
C(20):C(12)PC	734.1	29.4	34.0	33.2	1.05	11.6	37.8
C(22):C(12)PC	762.2	42.0	42.9	42.8	0.13	13.2	41.8
C(22):C(13)PC	778.2	42.6	44.4	44.1	0.35	14.1	44.5
C(8):C(18)PC	649.9	8.2	10.5	10.2	0.40	7.1	25.2
C(10):C(22)PC	734.1	34.8	38.4	37.3	0.88	12.2	39.2

[a] T_o and T_c are the onset and completion temperatures, respectively, of the thermal transition. $\Delta T_{1/2}$ is the transition width at half-maximal excess heat capacity. Other thermodynamic parameters (T_m, ΔH, and ΔS) are defined in the text.

Table II: Main Phase Transition Properties of Liposomes Prepared from Pure Symmetric Phosphatidylcholine

symmetric phosphatidylcholines	mol wt	calorimetric data of hydrated samples			literature values		
		T_m (°C)	ΔH (kcal/mol)	ΔS (eu/mol)	T_m (°C)	ΔH (kcal/mol)	ΔS (eu/mol)
C(14):C(14)PC	678.0	23.9	5.4	18.1	23.9[a]	5.4[a] 6.1[b]	18.2[a]
C(16):C(16)PC	734.1	41.4	8.6	27.3	41.4[a]	8.7[a] 8.5[b]	27.7[a]
C(18):C(18)PC	790.2	53.8	10.9	33.3	54.9[a]	10.6[a] 10.8[b]	32.3[a]
C(20):C(20)PC	846.3	64.2	13.2	39.1	64.7[c]	13.1[b]	

[a] Values taken from Mabrey and Sturtevant (1976). [b] Values calculated from the best-fit curve provided by Finegold and Singer (1986). [c] Value taken from Huang et al. (1982).

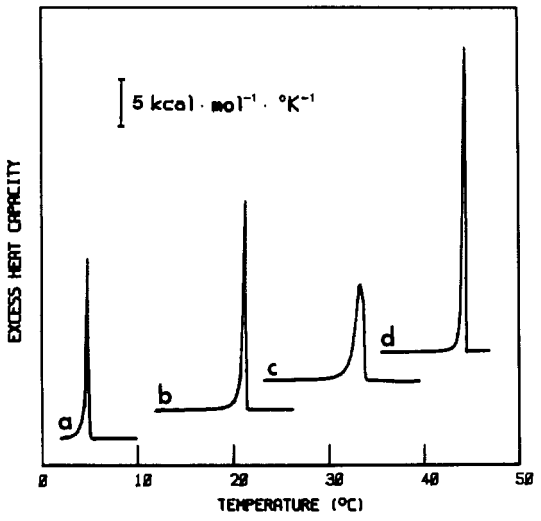

FIGURE 1: DSC thermograms for hydrated samples of (a) C(16):C(10)PC, (b) C(18):C(11)PC, (c) C(20):C(12)PC, and (d) C(22):C(13)PC. All scans were taken after the hydrated sample had been equilibrated at 0 °C for a minimum of a day. These are heating runs at 10 °C/h.

from those of nonhydrated samples. The transition temperatures and calorimetric enthalpies observed for the transitions of this series of fully hydrated phospholipids are summarized in Table I.

For comparison, the main phase transitions of multilamellar dispersions prepared from a series of pure symmetric phosphatidylcholines from C(14):C(14)PC to C(20):C(20)PC are also studied. The DSC results together with some literature values are summarized in Table II.

The total number of chain methylene units in C(20):C(12)PC and C(18):C(10)PC is identical with those in C(16):C(16)PC and C(14):C(14)PC, respectively. The endothermic transition profiles of these two pairs of lipid dispersions obtained under similar experimental conditions are presented in Figure 2A,B. Hydrated samples of C(16):C(16)PC preincubated at 0 °C for 3 days show multiple transitions at 16.5 (ΔH = 2.7 kcal/mol), 35.7 (ΔH = 1.3 kcal/mol), and 41.4 °C (ΔH = 8.6 kcal/mol); this behavior has been reported previously (Chen et al., 1980; Wu et al., 1985; Finegold & Singer, 1986). In contrast, each of C(20):C(12)PC samples prepared under the identical thermal protocol exhibits one broad asymmetric transition ($\Delta T_{1/2}$ = 1.0 °C) at 33.2 °C with a large ΔH (11.6 kcal/mol) as shown in Figure 2A. Comparison of C(14):C(14)PC with the appropriate C(18):C(10)PC also indicates that the thermal behavior of symmetric phosphatidylcholines is very different from that of asymmetric phosphatidylcholines. Hydrated samples of C(14):C(14)PC preincubated at 0 °C for 2 days exhibit two transitions at 14.5 °C (ΔH = 1.3 kcal/mol) and 23.9 °C (ΔH = 5.4 kcal/mol) as shown in Figure 2B, whereas hydrated C(18):C(10)PC samples after incubation at 0 °C for 2 days exhibit one symmetric but slightly broader transition ($\Delta T_{1/2}$ = 0.62 °C) at 19.2 °C (ΔH = 8.9 kcal/mol). This comparison again demonstrates that the transition enthalpy associated with the asymmetric phosphatidylcholines is considerably larger than that observed for the main transition of appropriate symmetric phosphatidylcholines. The transition entropy (ΔS) can be calculated from the ratio of $\Delta H/T_m$; the value of ΔS is thus significantly greater for samples of asymmetric phosphatidylcholine species (Tables I and II).

The phase transition temperatures of asymmetric phosphatidylcholine dispersions prepared from C(16):C(10)PC, C(18):C(11)PC, C(20):C(12)PC, and C(22):C(13)PC are plotted in Figure 3 as a function of the total number of carbon atoms in the two saturated acyl chains. It is evident that the values of T_m conform to a smooth curvilinear trend. Interestingly, a similar relationship is also observed with symmetric phosphatidylcholine dispersions, but the observed transition temperatures for the gel to liquid-crystalline transitions take place at correspondingly higher temperatures (Figure 3).

C(16):C(9)PC, C(18):C(10)PC, C(20):C(11)PC, and C(22):C(12)PC Assemblies. Since asymmetric C(18):C(10)PC molecules are known to form mixed interdigitated lamellae at $T < T_m$ (McIntosh et al., 1984; Hui et al., 1984), and since the normalized chain-length difference ($\Delta C/CL$) between the

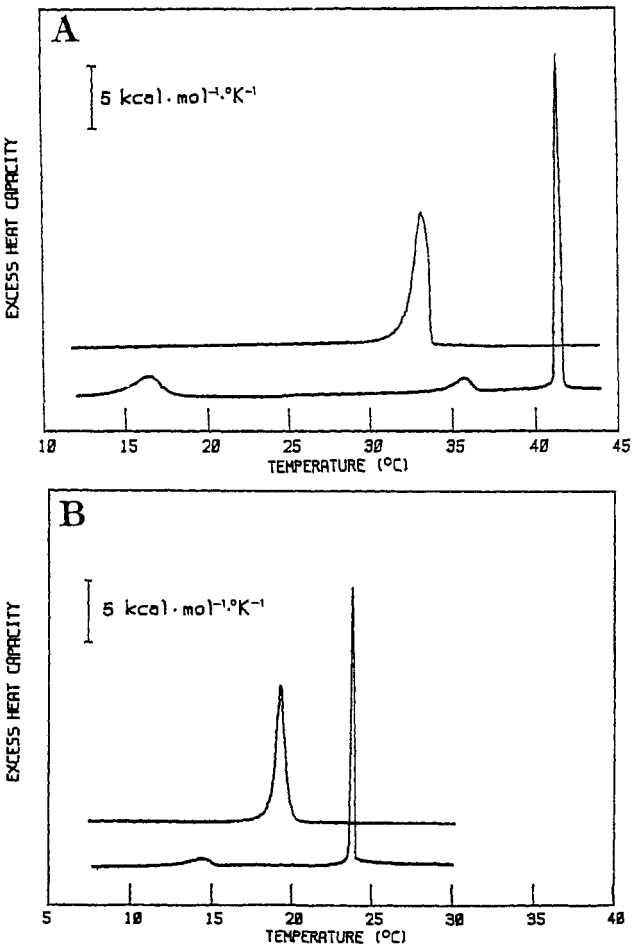

FIGURE 2: DSC heating thermograms of aqueous liposomes prepared from symmetric and asymmetric phosphatidylcholines with identical molecular weights. (A) Liposomes of 3.5 mM C(20):C(12)PC in 50 mM NaCl, 5 mM phosphate buffer, and 2 mM EDTA at pH 7.4 (upper curve) and of 3.3 mM C(16):C(16)PC in the same buffered NaCl solution containing 1 mM EDTA at pH 7.4 (bottom curve). Prior to DSC scans, each hydrated sample was incubated at 0 °C for 3 days. (B) Liposomes of 3.2 mM C(18):C(10)PC in 50 mM NaCl, 5 mM phosphate buffer, and 1 mM EDTA at pH 7.4 (upper curve) and of 4.1 mM C(14):C(14)PC in the same buffered EDTA–NaCl solution at pH 7.4 (lower curve). Scans were taken after each hydrated sample had equilibrated at 0 °C for 2 days. Scan rate: 10 °C/h.

sn-1 and *sn*-2 acyl chains for C(18):C(10)PC is 0.56, we have, therefore, synthesized a series of asymmetric phosphatidylcholines with ratios of $\Delta C/CL = 0.56 \pm 0.01$ and then compared their thermotropic behavior. These asymmetric phosphatidylcholines are C(16):C(9)PC, C(18):C(10)PC, C(20):C(11)PC, and C(22):C(12)PC, and their values of $\Delta C/CL$ are 0.57, 0.56, 0.55, and 0.55, respectively.

Similar to dispersions of asymmetric phosphatidylcholines with $\Delta C/CL = 0.50$, the thermotropic behavior of aqueous dispersions of this series of asymmetric phosphatidylcholines with $\Delta C/CL = 0.56 \pm 0.01$ was observed to be independent of the thermal history of the sample, i.e., how the sample was prepared. The DSC traces are characterized by single endothermic peaks with somewhat asymmetric shapes. The transition temperature (T_m) and calorimetric enthalpy of the transition (ΔH) are seen to increase progressively with increasing molecular weight of the phosphatidylcholine species. The thermodynamic parameters calculated from the endothermic transition profiles of this series of asymmetric phosphatidylcholines are summarized in Table I.

C(8):C(18)PC and C(10):C(22)PC Assemblies. The DSC results presented up to this point are confined to dispersions

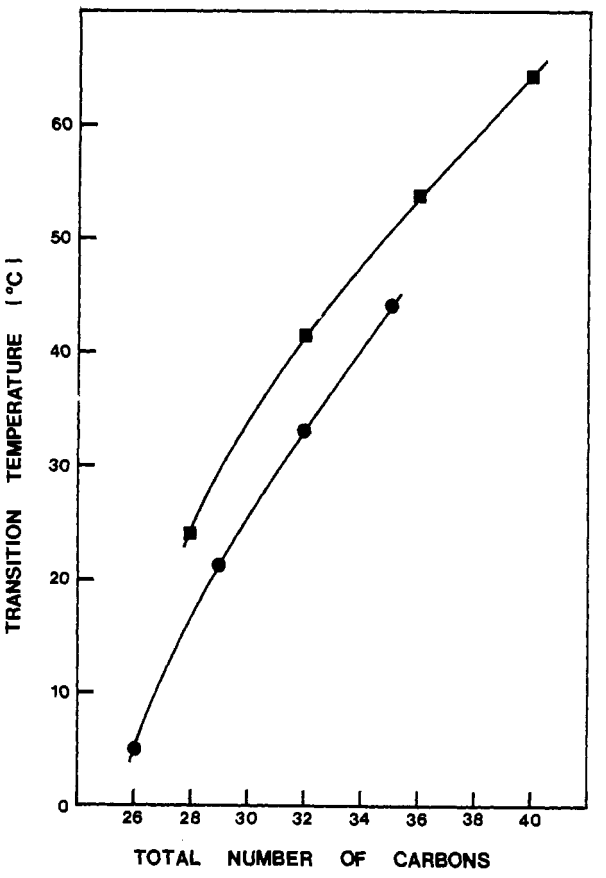

FIGURE 3: Phase transition temperature vs. the total number of carbons in the two acyl chains of various phosphatidylcholines. Closed circles: asymmetric phosphatidylcholines with $\Delta C/CL = 0.50$; C(16):C(10)PC, C(18):C(11)PC, C(20):C(12)PC, and C(22):C(13)PC. Closed squares: symmetric phosphatidylcholines; C(14):C(14)PC, C(16):C(16)PC, C(18):C(18)PC, and C(20):C(20)PC.

prepared from the asymmetric mixed-chain phosphatidylcholine species which carry a long saturated fatty acyl chain at the *sn*-1 position of the glycerol backbone and the normalized chain-length difference between the *sn*-1 and *sn*-2 acyl chains is either 0.50 or 0.56 ± 0.1. In order to check whether asymmetric mixed-chain phosphatidylcholines with the long acyl chain at the *sn*-2 position of glycerol will display thermotropic properties similar to those discussed earlier, we have exampled the phase behavior of C(8):C(18)PC and C(10):C(22)PC lamellae. Because of the bend of the initial *sn*-2 chain segment at the C(2) position, the apparent chain lengths of the longer acyl chains in the extended conformation (*CL*) for C(8):C(18)PC and C(10):C(22)PC are 15.5 and 19.5 C–C bond lengths, respectively, and the chain-length differences between the *sn*-1 and *sn*-2 acyl chains for C(8):C(18)PC and C(10):C(22)PC are 8.5 and 10.5 C–C bond lengths, respectively (Mason et al., 1981). The ratios of $\Delta C/CL$ for C(8):C(18)PC and C(10):C(22)PC can thus be calculated to be 0.55 and 0.54, respectively. For C(8):C(18)PC, a single sharp transition was observed to occur at 10.3 °C. The calorimetric enthalpy of this endothermic transition (ΔH) is 8.6 kcal/mol, and the half-height width ($\Delta T_{1/2}$) is 0.36 °C. The nonhydrated sample and the hydrated samples equilibrated at 0 °C for periods ranging from 1 to 24 h exhibit endothermic transitions with essentially identical values of T_m and ΔH. For C(10):C(22)PC, a single transition at 37.6 °C was observed; again, this transition behavior was virtually independent of the thermal history of the sample. The transition enthalpy is 15.2 kcal/mol, and the half-height width is 1.05 °C which is almost triple the width of the endothermic transition ob-

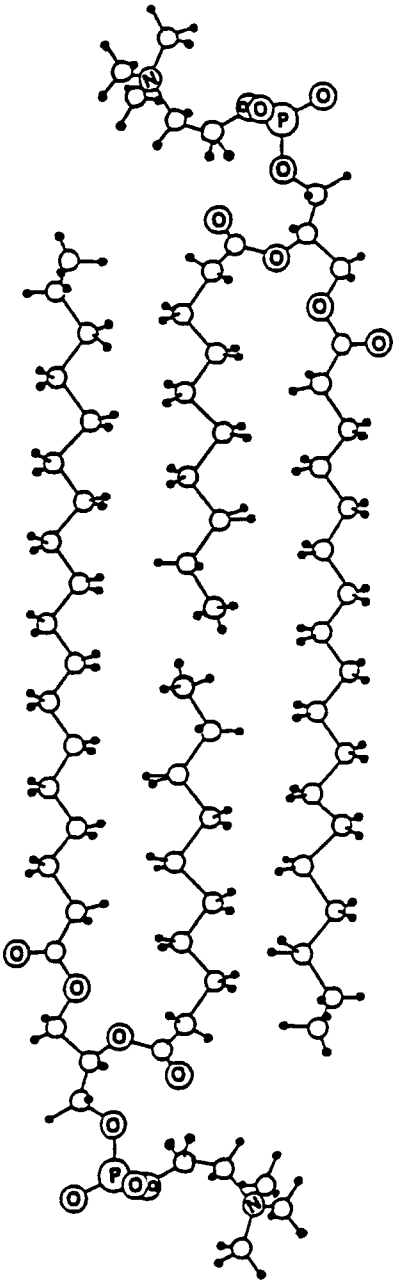

FIGURE 4: Schematic drawing to illustrate the acyl chain packing of C(18):C(10)PC in the mixed interdigitated bilayer. The C(18)-acyl chain is shown to interdigitate fully across the entire hydrocarbon width of the bilayer, while the C(10)-acyl chain meets end to end at the bilayer center with the C(10)-acyl chain from another C(18):C(10)PC molecule in the opposing bilayer leaflet. The effective chain-length difference between the C(18)- and C(10)-acyl chains in the gel-state bilayer (ΔC) is 9.5 carbon–carbon bonds, and the ratio of $\Delta C/CL$ is 0.56. The molecular conformation presented in this figure is adapted from the known phosphatidylcholine structure derived from X-ray single-crystal work of Pearson and Pascher (1979). The effective chain length for phospholipids discussed in the text, however, is based on neutron diffraction data obtained from phosphatidylcholine molecules in the gel-state bilayer (Zaccai et al., 1979).

served for C(8):C(18)PC dispersions.

Discussion

Prior to our discussion of the thermotropic properties of asymmetric phosphatidylcholine dispersions, it is appropriate to review briefly the structural model of bilayers composed of pure asymmetric C(18):C(10)PC at $T < T_m$ as evidenced by X-ray diffraction and freeze–fracture electron microscopy (McIntosh et al., 1984; Hui et al., 1984). The structural model

Table III: Apparent Chain Thickness of Asymmetric Phosphatidylcholine across the Hydrocarbon Width of the Mixed Interdigitated Bilayer

no.	asymmetric phosphatidylcholine	$\Delta C/CL$	apparent chain thickness in C–C bond length: one *sn*-1 chain or sum of two opposing *sn*-1 chains	apparent chain thickness in C–C bond length: sum of two opposing *sn*-2 chains or one *sn*-2 chain
1	C(16):C(9)PC	0.57	15	14.7
2	C(16):C(10)PC	0.50	15	16.7
3	C(18):C(10)PC	0.56	17	16.7
4	C(18):C(11)PC	0.50	17	18.7
5	C(20):C(11)PC	0.55	19	18.7
6	C(20):C(12)PC	0.50	19	20.7
7	C(22):C(12)PC	0.55	21	20.7
8	C(22):C(13)PC	0.50	21	22.7
9	C(8):C(18)PC	0.53	15.7	15.5
10	C(10):C(22)PC	0.53	19.7	19.5

is schematically shown in Figure 4 in which the long *sn*-1 acyl chain in a nearly all-trans conformation has a length of 17 carbon–carbon bonds orientated parallel to the bilayer normal and extended across the entire hydrocarbon width of the bilayer. The short *sn*-2 acyl chain has an effective chain length of 9 − 1.5 = 7.5 carbon–carbon bond lengths, where the reduction of 1.5 carbon–carbon bond lengths is due to the sharp bend of the *sn*-2 acyl chain at the C(2) atom (Zaccai et al., 1979). The effective thickness of two opposing *sn*-2 acyl chains in this model (Figure 4) is the sum of two 7.5 carbon–carbon bond lengths plus the close van der Waals contact distance between two opposing terminal methyl groups. The mean value of the minimum contact distance between the methyl–methyl groups in a protein such as hen egg white lysozyme is 3 Å (Levitt, 1974). In a gel-state bilayer, however, the distance could be considerably smaller. Pauling (1960) suggested that the van der Waals radius is about 0.8 Å greater than the corresponding single-bond radius, but the nonbonded radius in the direction along the covalent bond can be about 0.5 Å less. We can, therefore, estimate the closest contact distance between opposing terminal methyl groups in the gel-state bilayer to be about 2.14 Å, corresponding to about 1.7 carbon–carbon bond lengths along the axis of the bilayer normal. Consequently, the effective thickness of two opposing C(10)-acyl chains at the *sn*-2 position is about 16.7 carbon–carbon bond length which matches nearly perfectly with the 17 carbon–carbon bond length of the *sn*-1 acyl chain in the mixed interdigitated bilayer of C(18):C(10)PC at $T < T_m$.

Similar to the foregoing calculation for C(18):C(10)PC, the thickness of two opposing acyl chains at either the *sn*-1 or the *sn*-2 position in a mixed interdigitated bilayer for other asymmetric phosphatidylcholines can be estimated accordingly in terms of carbon–carbon bond lengths along the bilayer normal. The calculated values for various asymmetric phosphatidylcholines with $\Delta C/CL$ in the range of 0.50–0.57 are presented in Table III.

Before we discuss our DSC data, it is also pertinent to consider our Raman spectroscopic studies which show that the C(18):C(10)PC and C(14):C(14)PC lamellae, in excess water, exhibit similar inter- and intrachain disorders at 10 °C above T_m as evidenced by a common value (0.81) of the Raman peak height intensity ratio, $I(2935\ cm^{-1})/I(2884\ cm^{-1})$. In contrast, at 10 °C below T_m the values of $I(2935\ cm^{-1})/I(2884\ cm^{-1})$ obtained for C(18):C(10)PC and C(14):C(14)PC dispersions are 0.39 and 0.45, respectively (Huang et al., 1982, 1983), indicating that the hydrocarbon chains of the asymmetric C(18):C(10)PC are more ordered than the acyl chains of symmetric C(14):C(14)PC in the gel state. On the basis of

the Raman data, we can attribute the major difference between the symmetric and asymmetric phosphatidylcholines with an identical number of total methylene units to their lamellar packing in the gel state.

Now returning to the thermotropic phase behavior of multilamellar dispersions prepared from various pure phosphatidylcholines, the endothermic transition profiles of two pairs of symmetric and asymmetric phosphatidylcholines having identical molecular weight are compared in Figure 2. The transition profiles are clearly seen to be remarkably different. After the hydrated sample is incubated at 0 °C for 3 days, the C(16):C(16)PC dispersion, for example, exhibits multiple endothermic transitions at 16.5, 35.7, and 41.4 °C in the temperature range of 5–50 °C. In contrast, the hydrated C(20):C(12)PC sample after a 3-day incubation at 0 °C is detected by DSC to show a single endothermic transition at 33.2 °C. For C(20):C(12)PC, the single transition at 33.2 °C is independent of the thermal history of the sample, a characteristic well-known only for the main phase transition or the gel (P_{β}') to liquid-crystalline (L_{α}) phase transition at 41.4 °C for C(16):C(16)PC dispersions. The observed single transition for dispersions of all pure asymmetric phosphatidylcholine under study is, in fact, independent of the thermal history of the sample. These results thus suggest strongly that the single transition detected for asymmetric phosphatidylcholine dispersions corresponds to the gel to liquid-crystalline phase transition observed for dispersions of symmetric phosphatidylcholines.

The main transition temperatures of multilamellar dispersions prepared from saturated symmetric phosphatidylcholines of various chain lengths are well-known to be a continuous function of acyl chain length (Mabrey & Sturtevant, 1976; Silvius et al., 1979; Mason & Huang, 1981; Finegold & Singer, 1986). In Figure 3, the main transition temperature is plotted against the total number of carbon atoms in the two acyl chains. As expected, a smooth curve is observed for dispersions prepared from the saturated symmetric phosphatidylcholines. However, the data obtained from hydrated mixed-chain asymmeteric phosphatidylcholines with $\Delta C/CL$ = 0.5 fall on a different smooth curve, suggesting that the symmetric and asymmetric phosphatidylcholines may pack quite differently in their respective lamellae. In fact, the ΔH values associated with the gel to liquid-crystalline transition for saturated symmetric phosphatidylcholine dispersions are considerably lower than the corresponding values for dispersions of mixed-chain asymmetric phosphatidylcholines with identical molecular weight (Figure 2 and Tables I and II). The same holds true for the transition entropy (ΔS) in the process (Tables I and II). These thermodynamic results suggest strongly that the acyl chains of asymmetric phosphatidylcholines with $\Delta C/CL$ = 0.50 in the gel-state lamella are packed more orderly than those of symmetric phosphatidylcholines. The simplest molecular interpretation for the observed thermotropic behavior is that the asymmetric phosphatidylcholines with $\Delta C/CL$ = 0.50 are most likely packed at $T < T_m$ in a mixed interdigitated bilayer, which is known conformationally to be more ordered than the usual hydrated bilayer of symmetric phosphatidylcholines (McIntosh et al., 1984; Hui et al., 1984).

If asymmetric phosphatidylcholines with $\Delta C/CL$ = 0.50 do form, at $T < T_m$, mixed interdigitated bilayers in excess water, it is reasonable to assume a priori that the thermotropic properties of multilamellar dispersions of these phospholipids will be compatible with those of mixed interdigitated lamellae comprised of pure C(18):C(10)PC with $\Delta C/CL$ = 0.56.

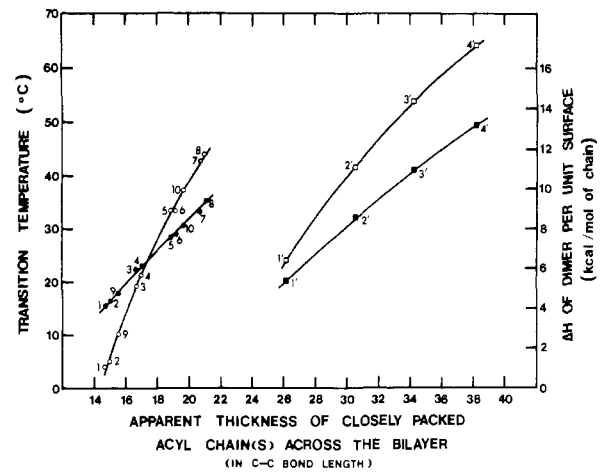

FIGURE 5: Transition temperature (T_m) and transition enthalpy (ΔH) vs. the apparent thickness of the laterally closely packed acyl chain(s) across the hydrocarbon width of the bilayer. The latter is taken from the smaller of the two values presented in Table III for asymmetric phosphatidylcholine, and from the formula $[2(n-1)-1.5]+1.7$ for symmetric phosphatidylcholine as discussed in the text. (●) ΔH of dimeric unit per unit surface for asymmetric phosphatidylcholine liposomes; (○) T_m for asymmetric phosphatidylcholine liposomes. The numbers 1–10 refer to various asymmetric phosphatidylcholines labeled in Table III. (■) ΔH for symmetric phosphatidylcholine liposomes; (□) T_m for symmetric phosphatidylcholine liposomes. The numbers 1′, 2′, 3′, and 4′ refer to data points derived from liposomes of C(14):C(14)PC, C(16):C(16)PC, C(18):C(18)PC, and C(20):C(20)PC, respectively.

Specifically, there seems a priori reason to expect that the thermodynamic data associated with the single phase transition of asymmetric phosphatidylcholines with $\Delta C/CL$ = 0.50 and 0.56 ± 0.1 would conform to a continuous function, if they are plotted against the proper acyl chain length.

For various asymmetric phosphatidylcholines packed in a mixed interdigitated bilayer, the length of the fully extended acyl chain which crosses the entire hydrocarbon width of the bilayer and the thickness of the two shorter acyl chains which meet end to end at the bilayer center are presented in Table III. The transition temperatures of liposomes prepared from these asymmetric phosphatidylcholines are plotted in Figure 5 as a function of the smaller of the two values presented in Table III. The experimental data fall nicely on a smooth curve in Figure 5, indicating that the a priori expectation discussed earlier is indeed borne out by the experimental results. Since the fundamental packing unit of asymmetric phosphatidylcholines in the mixed interdigitated bilayer is a dimer with a head-group area encompassing three hydrocarbon chains (Figure 4), the transition enthalpy of this dimeric unit per surface area in chain number is $2(\Delta H/3)$, where ΔH is the transition enthalpy per mole of phospholipid as tabulated in Table I. Values of $2(\Delta H/3)$ for various asymmetric phosphatidylcholines are plotted against the smaller of the values given in Table III. The data are clearly seen to fit to a smooth curve as shown in Figure 5. As expected, values of ΔS calculated from T_m and $2(\Delta H/3)$ for various asymmetric phosphatidylcholines under study also fall nicely on a smooth curve (data not shown). It should be emphasized that the thermodynamic parameter associated with the phase transition is plotted in Figure 5 against the smaller of the values given in Table III. The molecular basis is simple. Let us first consider the case that the length of the fully extended longer *sn*-1 acyl chain is slightly longer than the apparent thickness of the sum of two opposing shorter *sn*-2 acyl chains including the contact distance between the chain terminal methyl groups of the two opposing shorter chains. Here, a precise lateral chain–chain

contact interaction is dictated by the apparent thickness of two opposing *sn*-2 acyl chains. Because the cooperative melting of phospholipid acyl chains in the gel-state bilayer occurs within the hydrophobic region in which a close lateral chain–chain contact interaction exists, the thermodynamic parameters associated with the phase transition can be correlated to the sum of two opposing *sn*-2 acyl chains. Similarly, if the fully extended longer *sn*-1 acyl chain is slightly shorter than the apparent thickness of two opposing acyl chains at the *sn*-2 position, a precise lateral chain–chain van der Waals contact in the hydrocarbon interior of the gel state bilayer is not possible beyond the full length of the *sn*-1 acyl chain. Since the main phase transition of the bilayer reflects primarily the cooperative chain melting of the bilayer region with close lateral chain–chain interactions, the associated thermodynamic parameters (T_m, ΔH, and ΔS) can be correlated with the length of the *sn*-1 acyl chain.

Figure 5 also contains DSC data derived from asymmetric C(8):C(18)PC and C(10):C(22)PC dispersions. The experimental points indicated as 9 and 10 in Figure 5 fall nicely on the curve generated from DSC data obtained from lamellae of asymmetric PC in which the extended *sn*-1 acyl chain is about twice as long as the apparent length of the shorter *sn*-2 acyl chain. The good fit of all the experimental data to a smooth curve as seen in Figure 5 argues strongly that mixed interdigitated bilayers probably can be formed from all phospholipid species with ratio of $\Delta C/CL$ in the range of 0.50–0.56, irrespective of the position of the longer acyl chain at the glycerol backbone region.

For comparison, we have also studied the thermotropic behavior of liposomes prepared from various saturated symmetric phosphatidylcholines. The main transition temperatures of this series of saturated symmetric phosphatidylcholine dispersions are also plotted as a function of the total thickness of the apparent acyl chain lengths across the gel-state bilayer plus the closest contact distance between the two opposing terminal methyl groups or $[2(n-1)-1.5]+1.7$, where n is the number of carbons in the *sn*-1 or *sn*-2 acyl chain, $2(n-1)-1.5$ is the sum of the apparent chain lengths of two opposing acyl chains assuming that the *sn*-1 acyl chain of one lipid molecule is packed end to end with the *sn*-2 acyl chain of another lipid molecule in the opposing bilayer leaflet in the $P_{\beta'}$ phase, and the value of 1.7 is the closest contact distance in carbon–carbon bond lengths between the opposing chain methyl groups. The values of T_m or ΔH are seen to fall on a smooth continuous curve which, however, is distinctively separated from the curve plotted for asymmetric phosphatidylcholines as shown in Figure 5. Here the transition enthalpy (ΔH) equals the transition enthalpy of the dimeric packing unit in the bilayer per surface area in terms of chain number $[2(\Delta H/2)]$. By means of this figure, one can directly compare the thermodynamic properties of the geometrically identical bilayers in which the microscopic packing is different. Figure 5 does indicate that the main transition temperatures for symmetric phosphatidylcholine dispersions are actually lower than those of fully hydrated asymmetric phosphatidylcholines with $\Delta C/CL$ in the range of 0.50–0.57 at the corresponding effective thickness of acyl chains across the bilayer width. This extrapolated result is clearly consistent with a conclusion drawn from Raman and X-ray data that, in the gel state, the mixed interdigitated chain packing is more ordered than the usual hydrated normal bilayer.

At a temperature above T_m, C(18):C(10)PC forms a normal bilayer with two acyl chains per lipid head group; however, the two acyl chains are partially interdigitated in the liquid-crystalline state (McIntosh et al., 1984; Hui et al., 1984). It is worthy to mention that the C(18):C(10)PC bilayer is the first example in that acyl chain interdigitations are implied for phospholipid bilayers in the liquid-crystalline state. In this paper, we present calorimetric evidence to suggest that asymmetric phospholipids in which one acyl chain length is about twice as long as the other can form, at $T < T_m$, mixed interdigitated bilayers. By inference, these asymmetric phospholipids will also form partially interdigitated bilayers in the liquid-crystalline state. Hence, these asymmetric phospholipids not only are interesting but also are unique among all bilayer lipid species.

Due to the rather stringent requirement for the chain-length difference, the various asymmetric phospholipids under study may not be found at all in biological membranes. Consequently, the physiological significance for studying mixed interdigitated bilayers can be questioned. However, it should be mentioned that sphingolipids with a C(24)-acyl chain are commonly detected in biological membranes; these sphingolipids are characterized by having the ratio of $\Delta C/CL \simeq 0.5$, and they can assemble into mixed interdigitated bilayers at the physiological temperature (Levin et al., 1985). Another example is 1-palmitoyl-2-oleoyl-*sn*-glycero-3-phosphocholine which is probably the most abundant lipid species in mammalian membranes. In tissues or cells with slow or no turnover rate such as brain and red blood cells, 1-palmitoyl-2-oleoyl-*sn*-glycero-3-phosphocholine can undergo autoxidation leading to the scission of the cis double bond between C(9) and C(10) carbons in the *sn*-2 acyl chain. The resulting lipid is highly asymmetric with a chemical structure similar to C(16):C(9)PC. On the basis of data presented in this paper, C(16):C(9)PC can self-assemble into the interdigitated bilayer. Some biological membranes with increasing age may, therefore, have regions in which the normal noninterdigitated bilayer can be transformed into the interdigitated structure as induced by autoxidation. Understanding the various interdigitated structures of bilayers may, therefore, be useful in the delineation of the structure and function of biological membranes in general.

ACKNOWLEDGMENTS

We thank Dr. J. T. Mason for his advice in the synthesis of asymmetric phosphatidylcholines, J. L. Slater for technical assistance in plotting the DSC data, Dr. I. P. Sugar for critical comments on the manuscript, and F. L. Wilcoxen for expert typing.

REFERENCES

Chen, S. C., Sturtevant, J. M., & Gaffney, B. J. (1980) *Proc. Natl. Acad. Sci. U.S.A. 77*, 5060–5063.

Chowdhry, B. Z., Lipka, G., Dalziel, A. W., & Sturtevant, J. M. (1984) *Biophys. J. 45*, 901–904.

Finegold, L., & Singer, M. A. (1986) *Biochim. Biophys. Acta 855*, 417–420.

Hauser, H., Pascher, I., & Sundell, S. (1980) *J. Mol. Biol. 137*, 249–264.

Huang, C., Lapiedes, J. R., & Levin, I. R. (1982) *J. Am. Chem. Soc. 104*, 5926–5930.

Huang, C., Mason, J. T., & Levin, I. W. (1983) *Biochemistry 22*, 2775–2780.

Hui, S. W., & Huang, C. (1986) *Biochemistry 25*, 1330–1335.

Hui, S. W., Mason, J. T., & Huang, C. (1984) *Biochemistry 23*, 5570–5577.

Jain, M. K., Crecely, R. W., Hille, J. D. R., de Haas, G. H., & Gruner, S. M. (1985) *Biochim. Biophys. Acta 813*, 68–76.

Levin, I. W., Thompson, T. E., Barenholz, Y. B., & Huang, C. (1985) *Biochemistry 24*, 6282–6286.
Levitt, M. (1974) *J. Mol. Biol. 82*, 393–420.
Mabrey, S., & Sturtevant, J. M. (1976) *Proc. Natl. Acad. Sci. U.S.A. 73*, 3862–3866.
Mason, J. T., & Huang, C. (1981) *Lipids 16*, 604–608.
Mason, J. T., Huang, C., & Biltonen, R. L. (1981) *Biochemistry 20*, 6086–6092.
McDaniel, R. V., McIntosh, T. J., & Simon, S. A. (1983) *Biochim. Biophys. Acta 731*, 97–108.
McIntosh, T. J., Simon, S. A., Ellington, J. C., Jr., & Porter, N. A. (1984) *Biochemistry 23*, 4038–4044.
Pascher, I., & Sundell, S. (1986) *Biochim. Biophys. Acta 855*, 68–78.
Pascher, I., Sundell, S., Ebil, H., & Harlos, K. (1986) *Chem. Phys. Lipids 39*, 53–64.
Pauling, L. (1960) in *The Nature of the Chemical Bond*, 3rd ed., Cornell University Press, Ithaca, NY.
Pearson, R. H., & Pascher, I. (1979) *Nature (London) 281*, 499–501.
Ranck, J. L., & Tocanne, J. F. (1982) *FEBS Lett. 143*, 171–174.
Ranck, J. L., Keira, T., & Luzzati, V. (1977) *Biochim. Biophys. Acta 488*, 431–441.
Ruocco, M. J., Siminovitch, D. J., & Griffin, R. G. (1985) *Biochemistry 24*, 2406–2411.
Serrallach, E. N., Dijkman, R., de Haas, G. H., & Shipley, G. G. (1983) *J. Mol. Biol. 170*, 155–174.
Silvius, J. R., Read, B. D., & McElhaney, R. N. (1979) *Biochim. Biophys. Acta 555*, 175–178.
Wu, W., Chong, P. L., & Huang, C. (1985) *Biophys. J. 47*, 237–242.
Zaccai, G., Büldt, G., Seelig, A., & Seelig, J. (1979) *J. Mol. Biol. 134*, 683–706.

High-Resolution ^{1}H NMR Study of the Solution Structure of Alamethicin†

Gennaro Esposito,‡ John A. Carver,§ Jonathan Boyd, and Iain D. Campbell*
Department of Biochemistry, University of Oxford, OX1 3QU Oxford, U.K.
Received July 25, 1986; Revised Manuscript Received October 17, 1986

ABSTRACT: A ^{1}H NMR study of the peptide alamethicin, which forms voltage-gated ion channels in membranes, is described. The molecule was studied in methanol as a function of temperature and pH. A complete assignment of the spectra is given, including several stereospecific assignments. Alamethicin was found to have a structure substantially similar to the crystal although, in solution, the C-terminal dipeptide adopts a somewhat extended conformation. The overall conformation was insensitive to the ionization of the side chain of the only ionizable group, Glu-18.

Alamethicin is a linear icosapeptide that has antibiotic activity (Payne et al., 1970). It is extracted from the fungus *Trichoderma viride* as a mixture of related compounds, of which the main component has the following sequence (Gisin et al., 1977): Ac-Aib-Pro-Aib-Ala-Aib-Ala-Gln-Aib-Val-Aib-Gly-Leu-Aib-Pro-Val-Aib-Aib-Glu-Gln-Phol, where Aib[1] is α-aminoisobutyric acid [$(CH_3)_2C(NH_2)CO_2H$] and Phol is phenylalaninol, the α-amino alcohol derivative of phenylalanine.

Alamethicin forms voltage-gated ion channels in membranes (Mueller & Rudin, 1968; Fringeli & Fringeli, 1979, Lau & Chan, 1976; Banerjee et al., 1985). Two main classes of models have been proposed for the way in which this gated channel operates. These are the conformational change models and the helix dipole models. For example, Hall et al. (1984) proposed a conformational transition between a bent structure and a linear one as the basic gating event. This model is related to the one proposed by Fox and Richards (1982) although the "open" and "closed" states are not the same. Those models involving the helix dipole moment include those where the helix "flips" across the membrane and those where the helices in the channel move with respect to each other (Boheim et al., 1983; Mathew & Balaram, 1983; Edmonds, 1985).

These proposals for the action of the channel remain speculative since the structure of alamethicin in the lipid bilayer is unknown. In fact, there is conflicting evidence on its structure in the membrane since both an α-helical conformation (Boheim & Kolb, 1978) and a membrane-spanning β structure (Fringeli & Fringeli, 1979) have been reported.

Structural studies have, however, been carried out in various other solvents. The X-ray structure of alamethicin, crystallized from methanol (Fox & Richards, 1982), is predominantly helical. After the initial α-helix segment, Pro-14 introduces a bend that shifts the axis of the subsequent 3_{10} helix formed by the C-terminal residues. Circular dichroism studies (McMullen et al., 1971; Jung et al., 1975) showed a helix content ranging from 20% to 45% in a variety of organic solvents.

† This is a contribution from the Oxford Enzyme Group, which is supported by SERC.
* Author to whom correspondence should be addressed.
‡ Permanent address: Eniricerche spa, 32 00015 Monterotondo (Roma), Italy.
§ Present address: Department of Biochemistry, University of Adelaide, Adelaide, South Australia 5000, Australia.

[1] Abbreviations: NMR, nuclear magnetic resonance; 2D, two dimensional; DQF COSY, double quantum filtered correlation spectroscopy; NOESY, nuclear Overhauser enhancement spectroscopy; NOE, nuclear Overhauser effect; CYCLOPS, cyclic ordered phase scheme; ppm, parts per million; Hz/pt, hertz per point; Aib, α-aminoisobutyric acid; Phol, L-phenylalaninol; TSP, sodium 2,2,3,3-tetradeuterio-3-(trimethylsilyl)propionate; HPLC, high-performance liquid chromatography; rms, root mean square.

0006-2960/87/0426-1043$01.50/0